NeuroImage 89 (2014) 235–243

Contents lists available at ScienceDirect

NeuroImage

journal homepage: www.elsevier.com/locate/ynimg

Alpha activity reflects individual abilities to adapt to the environment

Jörn M. Horschig [a], Ole Jensen [a,*], Martine R. van Schouwenburg [a,b,c], Roshan Cools [a,b], Mathilde Bonnefond [a]

[a] Radboud University Nijmegen, Donders Institute for Brain, Behaviour and Cognition, 6525 EN Nijmegen, The Netherlands
[b] Radboud University Nijmegen Medical Centre, Department of Psychiatry, 6500 HB Nijmegen, The Netherlands
[c] Department of Neurology, University of California, San Francisco, CA 94158, USA

ARTICLE INFO

Article history:
Accepted 11 December 2013
Available online 19 December 2013

Keywords:
Alpha lateralization
Alpha modulation
Adaptation
Statistics
Oscillations
Covert attention
Attention switching
Magnetoencephalography
Individual differences

ABSTRACT

Recent findings suggest that oscillatory alpha activity (7–13 Hz) is associated with functional inhibition of sensory regions by filtering incoming information. Accordingly the alpha power in visual regions varies in anticipation of upcoming, predictable stimuli which has consequences for visual processing and subsequent behavior. In covert spatial attention studies it has been demonstrated that performance correlates with the adaptation of alpha power in response to explicit spatial cueing. However it remains unknown whether such an adaptation also occurs in response to implicit statistical properties of a task. In a covert attention switching paradigm, we here show evidence that individuals differ on how they adapt to implicit statistical properties of the task. Subjects whose behavioral performance reflects the implicit change in switch trial likelihood show strong adjustment of anticipatory alpha power lateralization. Most importantly, the stronger the behavioral adjustment to the switch trial likelihood was, the stronger the adjustment of anticipatory posterior alpha lateralization. We conclude that anticipatory spatial attention is reflected in the distribution of posterior alpha band power which is predictive of individual detection performance in response to the implicit statistical properties of the task.

Introduction

When driving down a long and lonesome road, you can probably attend to the road while also talking to your passenger. As you head towards a crowded crossing, you will gradually focus your attention to the traffic and eventually stop talking to your passenger. After having passed the crossing you can allow yourself to again attend to your passenger.

This example illustrates our ability to gradually adjust our attentional resources according to the surrounding. This process is likely to be associated with a gradual engagement and disengagement of brain regions processing respectively relevant or irrelevant for the task at hand. We hypothesize that this redistribution of resources is partly reflected by a differential adjustment of neural oscillations in various brain regions. Recent findings suggest that oscillatory alpha activity (7–13 Hz) plays a role in the distribution of attention resources by functional inhibition of sensory regions. This allows for filtering incoming information (reviewed in Bonnefond and Jensen, 2012; Foxe and Snyder, 2011; Jensen and Mazaheri, 2010; Jensen et al., 2012; Klimesch, 1999, 2012). The main idea is that alpha activity increases in sensory regions associated with suppression of task-irrelevant information, while alpha activity decreases in regions processing the task-relevant information. For instance, recent studies on visual covert attention have demonstrated that alpha power decreases in the parieto-occipital regions contralateral to the anticipated stimuli whereas alpha activity increases relatively in ipsilateral parieto-occipital regions (Worden et al., 2000). In a visuo-spatial detection task, Thut et al. (2006) demonstrated that the degree of prestimulus hemispheric alpha lateralization correlated with faster target detections. Kelly et al. (2009) and Händel et al. (2011) showed that the strength of prestimulus alpha lateralization is predictive of target discriminability. These studies indicate that hemispheric alpha lateralization correlates with enhanced performance in spatial attention tasks. Finally, Romei et al. (2010) demonstrated that TMS can be applied to entrain alpha oscillations over the parietal cortex ipsi-lateral to the attended direction. Since this entrainment had positive consequences for performance in a spatial attention task, one can argue for a causal inhibitory role of the alpha oscillations.

Two recent studies provided strong evidence for alpha power being under top-down control by demonstrating that prestimulus hemispheric alpha lateralization is influenced by explicit manipulation of the reliability of the spatial cue (i.e. a cue indicating the visual hemifield to covertly attend to). Haegens et al. (2011) conducted a spatial somatosensory discrimination task in which subjects were explicitly informed about the cue reliability. They found that the reliability of the cue correlated with the prestimulus alpha power lateralization in sensorimotor regions. A related study was performed by Gould et al. (2011) in the visual domain. They found a linear increase in alpha lateralization in visual regions with cue reliability. Furthermore, subjects with a stronger alpha power decrease contralateral to the cue also showed a stronger behavioral cueing effect as reflected in faster reaction times. These two studies show that alpha power in both visual and somatosensory

* Corresponding author at: Donders Institute for Brain, Cognition and Behaviour, Centre for Cognitive Neuroimaging, Radboud University Nijmegen, Kapittelweg 29, 6525 EN Nijmegen, The Netherlands.
E-mail address: o.jensen@donders.ru.nl (O. Jensen).

1053-8119/$ – see front matter © 2013 Elsevier Inc. All rights reserved.
http://dx.doi.org/10.1016/j.neuroimage.2013.12.018

regions is modulated by expectations about the likelihood of external events.

In these paradigms attention biasing was manipulated using explicit cues. In real life, however, attention biasing is often modulated by statistical properties of events in the environment. The aim of our current study was to assess whether biases in the allocation of attention due to statistical properties in the environment are reflected in anticipatory alpha-band lateralization. In a visual covert attention paradigm subjects were instructed to detect a stream of targets occurring in one hemifield. However, they had to switch attention to the unattended hemifield when a stimulus change occurred in the unattended side. The likelihood of an attention-switch-stimulus (indicating an attention switch trial) increased with the number of trials following the previous switch; however, the subjects were not explicitly informed about this statistical property. We assessed the individual change in alpha lateralization and switch-trial detection rate with switch-trial likelihood. Our study provides evidence that subjects who adapted their behavior (i.e. switch trial detection rate) according to the statistical properties of the task (switch-trial likelihood) also were the ones who adjusted their hemispheric alpha lateralization accordingly.

Materials and methods

Participants

Twenty healthy subjects with normal or corrected-to-normal vision (mean age: 24 ± (SD) 4 years) participated in the experiment after providing written informed consent according to the Declaration of Helsinki and the local Ethics board. The subjects did not have neurological or psychiatric disorders. The study was approved by the local ethics committee (CMO region Arnhem/Nijmegen).

Stimulus presentation and experimental paradigm

Stimulus presentation was performed using Presentation (Neurobehavioural Systems, Inc.) and a liquid crystal display video projector (SANYO PROxtraX multiverse; refresh rate of 60 Hz), back projecting onto a screen in the magnetically shielded room using two front-silvered mirrors. The distance to the screen as well as the size of the displayed screen size were measured individually for each subject. This allowed us to compute stimulus sizes and distances in visual degrees ensuring the same stimulus properties across subjects.

We developed a covert attention switching paradigm based on the study of van Schouwenburg et al. (2010), see Fig. 1. Squares were flashed on each side and subjects had to report the color of the attended square by a button press. When subjects detected a color change at the unattended side (signaling a *switch trial*), they had to report the color of the unattended square (but not the currently attended square) and switch attention to the unattended side in future trials.

At the beginning of each block, subjects were explicitly cued to which side to attend. From then on, the attended side was determined by stimuli properties alone. A central fixation point was presented during the entire experiment. Colored squares were flashed 1200 ms after the beginning of each trial for about 33 ms (two frames = 2/60Hz). These stimuli were presented with nine degrees eccentricity and two degrees lower than the fixation cross (measured from the fixation cross to the center of the stimuli). The squares were two degrees wide.

Subjects had to report the color of the square on the attended side by pressing a button with their left (for red) or right hand (for blue). On the unattended side, the square was either gray (*repeat trials*) or colored in blue or red (*switch trials*). Subjects had to respond within 2500 ms. After responding, the fixation cross turned gray, indicating that the subject could blink or move the eyes in a 1000 ms period. Then the fixation cross turned white again indicating the start of the next trial. Subjects had to keep attention to one hemifield (*repeat trial*) and report the color of the square on that side until they detected a colored stimulus

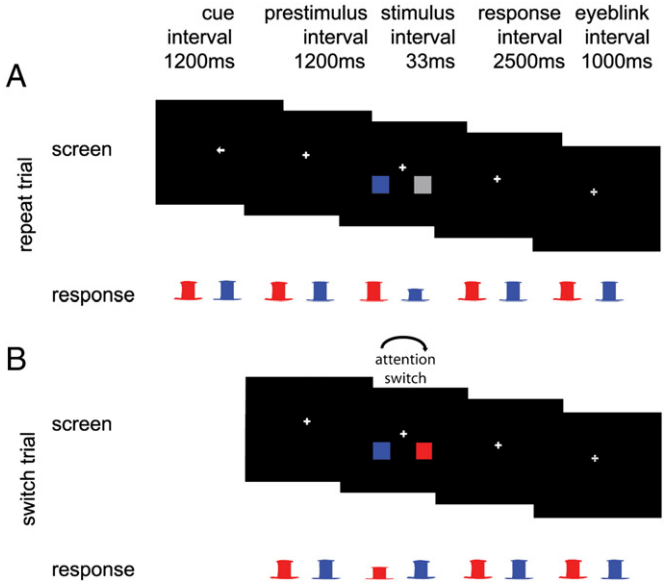

Fig. 1. The paradigm. The attended side was initially indicated by a cue. Subjects had to focus at the fixation cross and by button press indicate the color of the attended squares (left button for red and right button for blue). The 1200 ms prestimulus period was followed by the colored stimuli flashed for 33 ms. Subjects had to respond within 2500 ms. If there was a color change in the square of the unattended hemifield, attention had to switch to that direction ('switch-trial'). After the response there was a 1000 ms window for eye blinking. A Example of an explicit cue followed by a repeat trial. The subject had to covertly attend to the left and subsequently report the color of the stimuli by pressing the corresponding button (here: blue, right button). B Example of a switch trial. In the previous repeat trials, the subject had to attend to the left, because of the initially shown spatial cue. Upon stimulus presentation, the subject correctly switched attention and indicated so by reporting the color of the stimulus at the formerly unattended side (here: right, red color). If the subject responded according to the formerly attended side (here: left, blue), the switch trial would repeat up to four times. Repetitions of switch trials were removed from the analysis. If the subject did not switch after the fourth consecutive switch trial, another explicit spatial cue pointing to the formerly unattended side was presented (here: a rightward pointing arrow).

in the unattended hemifield (switch stimulus). A trial which includes a switch stimulus is called a *switch trial*. The switch stimulus was detected if the color of the unattended target was correctly reported (*detected switch trial*). Subjects then had to keep attending the formerly unattended hemifield until a next switch trial was detected. If a subject failed to detect the switch stimulus (*undetected switch trial*), it was repeated with a random color (blue or red) up to four times. We focused the analysis on the first switch trials, i.e. dismissed switch trials immediately following an *undetected switch trial*.

The probability of a switch trial was increasing with the number of trials since the last switch trial (see Fig. 2). The number of trials between switches was precomputed, so that the sequence of trials was as similar as possible across different subjects (on average 4.5 trials). We call the number of trials from the last switch trial *Inter-Switch Trial Number* (ISTN). A number of *detected repeat trials* were required to trigger a switch trial. When a subject made a wrong response to a repeat trial, the trial number from the last switch trial was reset. Thus a number of consecutive correct responses to repeat trials were needed to trigger a switch trial. This ensured that subjects did not only attend the supposedly unattended side throughout the experiment. The number of response errors to repeat trials was, however, very low (<10%, see also Section 3.1 Behavioral Performance). Our setup resulted in a linear increase in switch trial likelihood with ISTN (see Fig. 2). Subjects were given a break of at least 2.5 s after every 15th *detected switch trial*. After each break, an explicit spatial cue indicated the initially attended side. Additional explicit spatial cues were provided after four *undetected switch trials* and after four errors to repeat trials in between two switch trials (5.2 ± (SD) 3.9 cues for attention to the left and 5.9 ± (SD) 4.4

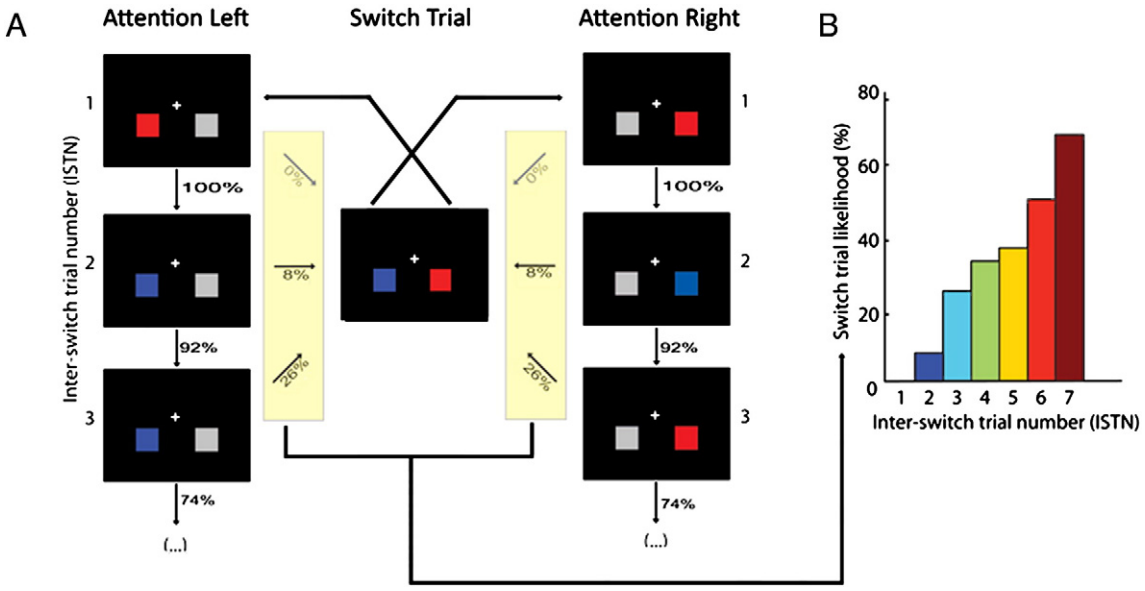

Fig. 2. Relation between switch-trial occurrence and Inter-switch trial number (ISTN). A The likelihood that a switch trial would occur (i.e. the hazard rate) was independent of the attended side, but increased as function of trials since the last switch trial. More repeat trials since the last switch trial made it more likely that the next trial could be a switch trial. B The likelihood of switch trial occurrences (i.e. the hazard rate) linearly increased with ISTN.

cues for attention to the right). The experiment was terminated after the first *detected switch trial* 60 min after the experiment began.

In order to make the task sufficiently difficult, the intensity of the stimuli was varied across subjects and trials in an adaptive staircase-like procedure on a 20-step scale (1: darkest; 20: brightest), starting at 10 for both the neutral and the colored stimuli. This was done in the first block (i.e. until the 15th *detected* switch trial). The intensities of the neutral and colored stimuli were modulated according to different criteria. Repeat trials should be sufficiently demanding while keeping response errors as low as possible. Therefore we kept reducing the brightness of the colored stimuli to a level in which the subject could perform the discrimination with no errors. The color intensity was reduced by one step after each *detected switch trial* and if no errors to repeat trials were made before. After a response error to repeat trials, the intensity was increased by one step again. The intensity of the neutral stimulus was adapted to manipulate the difficulty of switch trials. A large intensity difference between colored and neutral stimuli makes detection of switch trials easier (pop-out effect), whereas a similar intensity results in a harder task and less detected switch trials. We aimed at a correct response rate to switch trials between 25% and 75%. After a detected switch trial, the neutral stimulus was increased in intensity by one when less than 25% of all switch trials were detected. The intensity was decreased by one step when more than 75% of all switch trials were detected. The twenty levels of stimulus luminance were visually and mathematically matched according to the CIELAB specifications (Rubner et al., 1998; Ruzon and Tomasi, 1999). This procedure resulted in similar intensities across most subjects. Subjects 4, 7 and 18, however, were exposed to a brighter neutral stimulus (levels 11, 9 and 9, respectively, versus levels 2 or 3). Subjects 4 and 7 were also exposed to brighter colored stimuli (contrast levels 9 and 6 versus 1 to 4). These subjects showed no differences in behavioral performance compared to all other subjects and were thus included in further analysis. Note that the adaptation procedure was only done in the first block until the 15th detected switch trial. Trials from this block were not included in the analyses.

Prior to the experiment, participants received written and verbal task instructions. Subjects were instructed to prioritize accuracy rather than speed, but were informed that they should respond within 2.5 s. They were instructed to detect the color at the cued side, but switch attention to the uncued side if the color at that side turned from gray to either blue or red. Subjects were informed that they would receive no response feedback. The instructions did not inform about the task statistics. After the instructions, subjects had to complete a short tutorial on the computer, which explained the paradigm and introduced the stimuli. To diminish learning effects, subjects performed a short test run in a separate, acoustically shielded room. The test run had exactly the same properties as the final experimental run and included 30 *detected switch trials* (approximately 10 min). Afterwards, participants were seated upright in the MEG system in a comfortable position. They were instructed to sit as still as possible while fixating centrally. In our analysis, as already reported above, we discarded all trials up to the first experimental break.

Data acquisition

The ongoing brain activity was recorded using a whole-head MEG system with 275 axial gradiometers (CTF MEG Systems, VSM MedTech Ltd.) at a sampling frequency of 1200 Hz. After acquisition, data were resampled at 600 Hz. During the experiment, the subject's head position was continuously recorded using three coils, one placed at each ear canal (mounted on earplugs) and one at the nasion (Stolk et al., 2013). When the subject's head moved such that any coil was more than 2.5 mm away from its initial position, the head was realigned during the next break. In addition, an EyeLink 1000 eyetracker (http://www.sr-research.com) was used to track potential saccades.

Additionally, we acquired individual, high-resolution anatomical images using a 1.5 T Siemens Magnetom Sonata system (Erlangen, Germany) with 1 mm isotropic voxel size. To co-register the MEG and anatomical MR data, we used the same earplugs as in the MEG measurement with additional vitamin E capsules during the anatomical scan.

Data analysis

We computed the response rate to repeat trials (*number of detected repeat trials* divided by *total amount of repeat trials*), the switch-rate (*number of detected switch trials* divided by *total amount of switch trials*) and the mean reaction time (*RT*) to repeat and switch trials. Further, we separated trials into seven bins according to the number of trials from

the last switch trial (i.e. according to the inter-switch trial number, ISTN). Trials after the seventh ISTN bin were dismissed from further analysis since the number of trials was too little for further analysis (less than 16 trials). Also, we dismissed switch trials that immediately succeeded an *undetected switch trial*, i.e. we only analyzed *switch trials* that were preceded by at least one *repeat trial*. Note that the switch trial likelihood for the first ISTN bin is zero, thus there are no measures of switch trials in ISTN bin 1. All results are reported in the format of sample mean ± standard deviation.

The MEG data were analyzed using the Matlab-based FieldTrip toolbox, developed at the Donders Institute for Brain, Cognition and Behaviour (Oostenveld at al., 2011). Artifacts were detected in a semi-automatic fashion, which included visual inspection and trial rejection based on variance and other measures as implemented in FieldTrip. We focused artifact rejection in the window from −1 s to 0.5 s relative to stimulus onset. We excluded trials in which the head position exceeded 5 mm from the average position throughout the experiment. Based on the eye-tracker data, we excluded trials with eye saccades exceeding 3 visual degrees from the fixation cross or eye blinks. On average around 29% of the trials were excluded, mainly because of eye blinks or movements. For the sensor-level analysis, the combined planar gradients of the MEG field distribution were estimated using a nearest neighbor procedure, similar to the method described by Bastiaansen and Knösche (2000).

Spectral analysis

We computed the time-frequency representations (TFRs) of power from 2 to 32 Hz (1 Hz increments) for each trial from a −1.0 s to 0.5 s interval around the stimulus onset. Spectral content was estimated using an adaptive sliding window of four cycles per frequency bin (e.g. $\Delta t = 400$ ms for 10 Hz), which was multiplied with a Hanning window prior to applying a fast Fourier transform. For further analyses, we computed the non-time resolved power spectrum from −1 s to 0 s using a Hanning-tapered Fast Fourier Transform. This time-period was chosen because our main hypothesis pertained to anticipatory processes. From these power spectra we extracted power in the individual alpha-band (see below) at the sensors of interest.

Alpha modulation index computation

We will refer to the alpha modulation as the difference of power in the alpha-band between trials in the condition attention left and attention right in the prestimulus interval. For each subject we calculated the alpha modulation index (AMI) defined as follows:

$$\mathrm{AMI_L} := \log\left(\frac{\overleftarrow{\alpha_L}}{\overrightarrow{\alpha_L}}\right) \;;\; \mathrm{AMI_R} := \log\left(\frac{\overleftarrow{\alpha_R}}{\overrightarrow{\alpha_R}}\right)$$

$$\mathrm{AMI} := \mathrm{AMI_L} - \mathrm{AMI_R} = \log\left(\frac{\overleftarrow{\alpha_L}}{\overrightarrow{\alpha_L}}\right) - \log\left(\frac{\overleftarrow{\alpha_R}}{\overrightarrow{\alpha_R}}\right) = \log\left(\frac{\overleftarrow{\alpha_L}\overrightarrow{\alpha_R}}{\overrightarrow{\alpha_L}\overleftarrow{\alpha_R}}\right)$$

$$= \log\left(\frac{\overleftarrow{\alpha_L}}{\overleftarrow{\alpha_R}}\right) - \log\left(\frac{\overrightarrow{\alpha_L}}{\overrightarrow{\alpha_R}}\right).$$

Here, α denotes power in the alpha-band. The subscripts L and R denote the sensors of interest over the left and right hemisphere, respectively. The arrow above α denotes the condition, namely attention left and attention right. Thus, $\overrightarrow{\alpha}_L$ and $\overrightarrow{\alpha}_R$ denote alpha-band power in the sensors of interest over the left and right hemisphere, respectively, in the average of all attention right trials. $\overleftarrow{\alpha}_L$ and $\overleftarrow{\alpha}_R$ denote the equivalent with respective attention to the left hemifield. These AMI measures reflect the modulation of alpha band activity with respect to spatial attention to the left and the right. When comparing attention to the left versus the right, $\mathrm{AMI_L}$ will be positive, and the $\mathrm{AMI_R}$ will be negative. This corresponds to a relative ipsilateral increase and contralateral decrease in alpha power. Thus, a positive AMI reflects the degree of hemispheric lateralization and thus attention toward the attended side (cf. Gould et al., 2011; Haegens et al., 2011; Thut et al., 2006). A negative AMI reflects a high degree of attention to the side where the switch stimulus will appear. The attended side changed after each *detected switch trial*.

In order to optimize the sensitivity of the analysis, we focused the analysis on the band around the individual alpha frequency (IAF, Klimesch, 1999) to which we will refer to as the individual alpha-band (Thut et al., 2006). The IAF is determined by the peak frequency in the 7–13 Hz spectrum. The individual alpha-band is defined from 4 Hz below to 2 Hz above the IAF. The average peak frequency across subjects was 10.5 Hz ± (SD)0.64 Hz, which is ~1.5 Hz lower than what Worden et al. (2000) and Thut et al. (2006) reported, but close to the findings of Sauseng et al. (2005).

To define the sensors of interest for pre-stimulus analyses, we computed the relative difference in alpha-band power induced by the stimulus (0 to 0.5 s, see Fig. 4A) between attention left and attention right trials for all *repeat trials*. We selected twelve sensors with the strongest positive induced response and twelve sensors with the strongest negative induced response for the left versus right attention contrast. These sensors will be referred to as the left and right regions of interest (ROI), which were subsequently used to compute the $\mathrm{AMI_L}$, $\mathrm{AMI_R}$ and AMI per ISTN.

To assess individual differences in performance, we performed a linear trend analysis on the above mentioned binning scheme (ISTN), expecting a linear relationship between the ISTN, AMI and behavioral measures. We restricted the analysis to a linear trend, because a linear relationship between explicit instruction cues and behavioral and neural measures was found by Gould et al. (2011) and Haegens et al. (2011). Moreover, we also computed a within-subject linear regression between these measures.

Source analysis

We used a beamforming approach based on an adaptive spatial filtering technique (Dynamic Imaging of Coherent Sources, DICS) to localize the underlying sources of the alpha band activity (Gross et al., 2001; Schoffelen et al., 2008). The subject specific anatomical brain scans were discretized with a resolution of 1 cm. We used a realistically shaped single shell head model based on the subject specific anatomical MRI to compute the leadfield per grid point (Nolte et al., 2003). The beamforming algorithm computes a spatial filter per grid point using the cross-spectral density matrix obtained from a Fourier transform. We computed the cross-spectral density matrix based on the interval from −1 s to 0 s relative to stimulus onset. The Fourier spectrum was centered on 10 Hz computed using five Slepian tapers (Percival and Walden, 1993), i.e. a 3 Hz smoothing, resulting in an estimate of 7–13 Hz. To allow averaging over subjects, we normalized subject individual head models by inversely warping it to the MNI template brain (International Consortium for Brain Mapping, Montreal Neurological Institute, Canada) using SPM8 (http://www.fil.ion.ucl.ac.uk/spm). Based on all trials a spatial filter was computed, which we used to estimate source activity of attention left and attention right trials separately.

Statistical analysis

Statistical analysis of behavioral data was performed using a repeated measured analysis of variance (ANOVA) using the factors trial type (repeat or switch trial) and attended hemifield (left or right). For analysis of reaction times, we additionally included the correct response rate as a factor. Further behavioral analyses were conducted using paired *t*-test.

Statistical significance of neural data was assessed using a non-parametric cluster-based permutation test (Maris and Oostenveld, 2007). In the cluster-based permutation test, notational significant

clusters in channel/grid space are detected using a parametric test-statistic, here the t-statistic thresholded by an uncorrected p-value (0.05 for sensor level data and 0.025 for source level analysis to get spatially more defined cluster). Then values in channel/grid tiles are reshuffled randomly between the conditions and the maximum cluster size per permutation is stored to assess the distribution of maximal cluster sizes. Cluster size is defined as the sum of the t-values in that cluster. Cluster significance in the original contrast is assessed by comparing their cluster size with the distribution of the maximal cluster sizes across permutations. A cluster-based permutation test therefore controls for multiple comparisons. We considered a cluster to be significant at alpha = 0.05 (two-sided), thus if the cluster size lies above or below 2.5% of the permutation distribution. To determine the regions of interest, we averaged over time and frequency of interest (here −1 s to 0 s, and 7 Hz to 13 Hz) to yield clusters in channel/grid space. 2000 permutations were used to estimate the distribution of maximal cluster sizes on sensor level; 5000 permutations were used for the source level data.

Results

Behavioral performance

The subjects were asked to perform the task described in Fig. 1. We recorded 1018 ± 98 (mean ± standard deviation) trials per subject and 722 ± 122 trials were left after artifact rejection; 151 ± 21 of them were *switch trials*, i.e. trials which include a switch stimulus (see Section 2.2). We expected the detection of switch trials to be more difficult than the detection of repeat trials, i.e. to be associated with longer reaction times and more errors (van Schouwenburg, 2010). Figs. 3A and D provide an overview of the behavioral data for respectively response rates and reaction times. A 2-by-2 ANOVA on response rates with the factors attended hemifield (left or right) and trial type (repeat or switch trial) revealed a main effect of trial type ($F(1, 77) = 72.88$, $p < 0.01$). On average, subjects responded correctly to 91.2 ± 4.6% of all repeat trials and detected 64.2 ± 18.7% of all switch trials

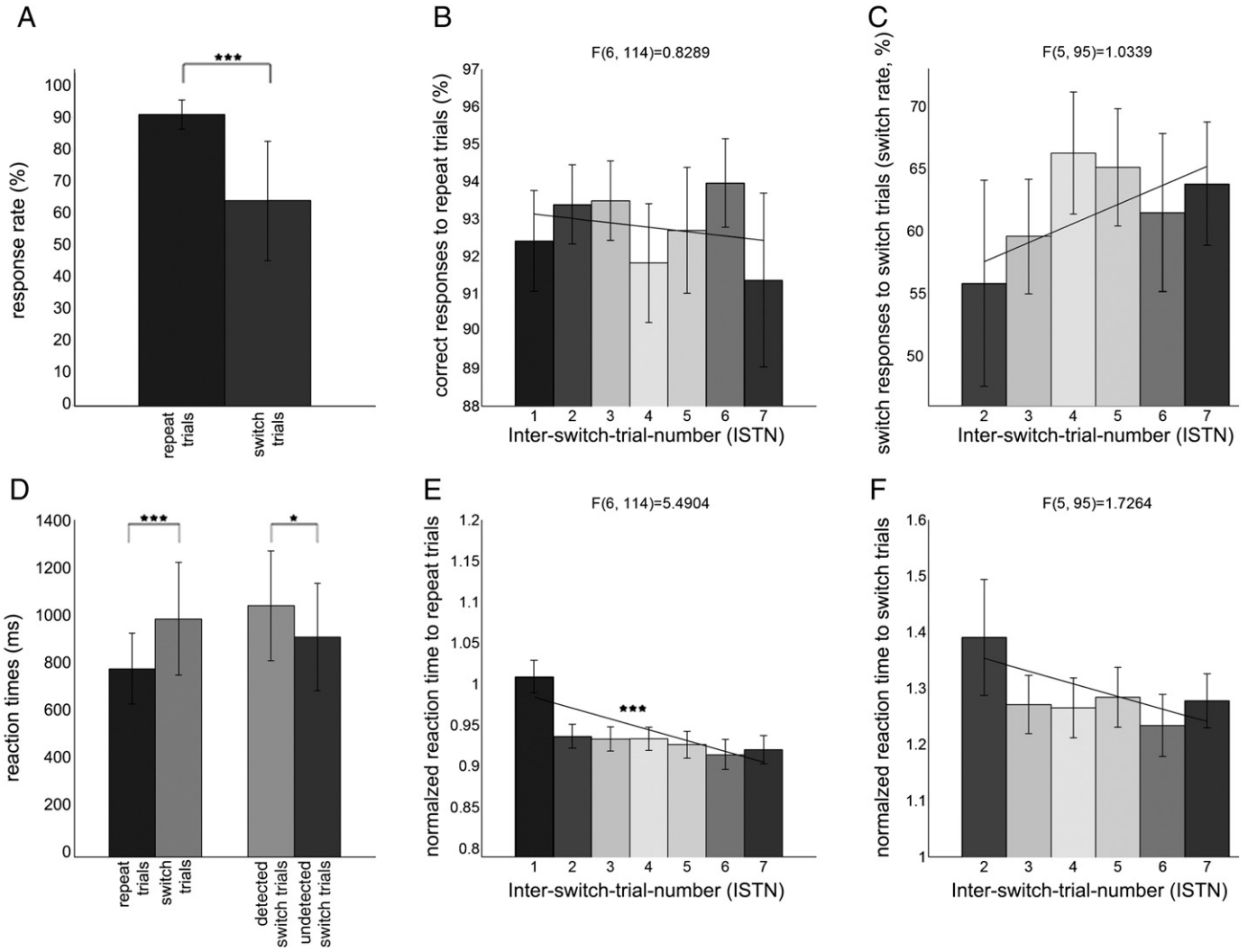

Fig. 3. Behavioral results. A Mean rate of correct responses to repeat and switch trials averaged over all subjects and ISTN bins. The correct response rate was lower for switch trials than for repeat trials ($F(1, 77) = 72.88$, $p < 0.01$) B There was no significant linear trend over ISTN bins in terms of correct responses to repeat trials ($F(6, 114) = 0.8289$, $p = 0.55$). C There was no significant linear trend over ISTN bins with switch-rate ($F(5, 95) = 1.0339$, $p = 0.40$). Note that the paradigm was designed so that there were no switch trials in ISTN bin 1; therefore the linear trend analysis starts at ISTN bin 2. D Reaction times to repeat trials were significantly lower than to switch trials ($F(1, 153) = 14.93$, $p < 0.01$). A post-hoc *t*-test indicated that responses to detected switch trials were faster than to undetected switch trials ($t(19) = 3.55$, $p < 0.01$, *uncorrected*) E There was a significant negative linear trend for reaction time to repeat trials over ISTN bins ($F(6, 114) = 5.54904$, $p < 0.01$). A trend analysis without the first ISTN bin showed no significant trend anymore ($F(5, 95) = 0.6585$, $p = .66$). F There was no significant linear trend between reaction times to switch trials and ISTN bins ($F(5, 95) = 1.7264$, $p = 0.14$). Horizontal lines depict the within-subject regression line. For illustration purposes, reaction times were normalized by the average reaction time of all trials per subject before averaging across subjects. *** indicates a significant effect with $p < 0.01$, * indicates a significant effect with $p < 0.05$.

(*switch-rate*) resulting in 105 ± 20 detected switch trials. We did not find a significant effect of hemifield ($F(1, 77) = 0.01$, $p > 0.9$) or a significant interaction between the two factors ($F(1,77) = 0.14$, $p > 0.7$).

To quantify the reaction time effects, we conducted a 2-by-2-by-2 ANOVA with the factors attended hemifield (left or right), trial type (repeat or switch trial) and correctness of response. A significant main effect of trial type ($F(1, 153) = 14.93$, $p < 0.01$) revealed that subjects responded significantly slower to switch trials (995 ± 234 ms) than to repeat trials (787 ± 148 ms). There was no main effect of hemifield ($F(1, 153) = 0.68$, $p > 0.4$). Furthermore, there was a significant interaction between trial type and correctness of response ($F(1, 153) = 27.35$, $p < 0.01$). Using a post-hoc *t*-test we found that reaction times to detected switch trials were significantly longer than to undetected switch trials (difference: 131 ± 165 ms, $t(19) = 3.55$, $p < 0.01$, *uncorrected*), while reaction times to repeat trials were significantly slower for correct responses than for errors (−251 ± 147 ms, $t(19) = 2.73$, $p < 0.05$, *uncorrected*). We conclude that responses to switch trials required more effort than to repeat trials, independently of the attended hemifield, as reflected in increased reaction times and reduced response rates.

The main focus of the study pertained to how subjects adapted to implicit changes in switch trial likelihood determined by the inter-switch-trial-number (ISTN), i.e. the number of trials from a previous switch trial (see Section 2.4). See Table 1 for an overview of the amount of trials per ISTN bin. For an overview of the grand average over subjects, see Figs. 3B and C for repeat trials and E and F for switch trials.

Subjects showed a linear decrease in reaction time for repeat trials ($F(6, 114) = 5.4904$, $p < 0.01$) with ISTN, but this was entirely driven by the first ISTN bin following attention switches. A trend analysis without the first ISTN bin showed no significant trend anymore ($F(5, 95) = 0.6585$, $p = .66$). We interpret as an attention switch cost effect (see e.g. Monsell, 2003) after subjects reallocated spatial attention and therefore adjusted to task changes. Because of the observed attention switch cost and because ISTN bin 1 has no switch trials, we conducted all subsequent analyses from ISTN bin 2 onwards. For switch trials, we hypothesized that the subjects' performance would be relatively low for early and thus unexpected switch trials and but gradually improve for later switch trials. In the grand average, we did not, however, find a linear trend between ISTN bin and detection rate of switch trials ($F(5, 95) = 1.0339$, $p = 0.40$). There were no other significant effects in the grand average. Thus, in the data averaged over subject, we did not find proof of behavioral adjustments to the task statistics.

Prestimulus alpha modulation

We next considered the neuronal mechanism of anticipatory attention as characterized by hemispheric specific alpha band modulations. In our main analysis, we focused on the alpha-modulation index (AMI) by contrasting the alpha power between contra- and ipsilateral attention for each hemisphere separately and in combination (see Section 2.6).

Figs. 4A and B show the topographic distribution of the alpha band modulation, i.e. alpha-band power (7–13 Hz) per sensor when contrasting attention left and attention right trials. To determine the sensors of interest for later analysis on the pre-stimulus interval, we selected sensors with the strongest induced response to the stimuli in repeat trials in the alpha band. The twelve left sensors showing the strongest positive stimulus induced alpha modulation and the twelve right sensors showing the strongest negative induced alpha modulation (Fig. 4A, marked with asterisks) were selected for further analysis to compute the alpha modulation index (AMI). We will refer to these as regions of interest (ROI). The remaining analyses were performed in the prestimulus interval (depicted in Figs. 4B, C and D). We performed a source-reconstruction analysis in the prestimulus interval (−1 s to 0 s) and in the alpha-band (7–13 Hz). The analysis on source-level confirmed a significant left parieto-occipital power increase (Fig. 4C; cluster-based permutation test, $p < 0.05$).

To verify whether the alpha band activity was modulated by attention in the prestimulus window, we performed a cluster-based permutation test over all sensors. We found one significant cluster over left parieto-occipital regions in the contrast attention left versus attention right ($p = 0.02$). This cluster included eight of the twelve pre-selected left ROI channels, confirming the appropriateness of the selected ROI. In the right hemisphere sensors we did not find evidence for significant anticipatory alpha band modulation with attention. Fig. 4D shows the time-frequency representation of the left and right ROIs for the contrast attention left versus attention. In line with the cluster-based permutation statistics, alpha power appears higher in the left ROI for attention left compared to attention right. As expected the time-frequency decomposition shows induced, lateralized activity around 10 Hz at ~200 ms after stimulus onset.

Next, we asked whether the ability to detect switch trials correlated with the magnitude of alpha power over the left or right ROI. We tested whether there was a difference between detected and undetected switch trials when considering the left minus right attention condition (independent of ISTN bin). We did not find significant differences neither for the pre- nor for the poststimulus period (cluster-based permutation test, all $p > 0.1$).

Individual behavioral and neural adaptation to switch trial likelihood

The likelihood that the next trial would have a switch trial increased with ISTN, i.e. with the number of trials since the last switch trial (see Fig. 2). We expected subjects to adapt to the implicit change in switch trials likelihood, which will be reflected in behavioral and neural adaptation. As already reported (Section 3.1), we did not find a systematic increase in detection rate with increasing ISTN on grand average level. Next, we computed the power spectra for the trials in each ISTN bin in the prestimulus interval and subsequently computed the AMI (the alpha modulation combined over the left and right ROI; see Section 2.6) per ISTN bin. In this analysis we neglected the first ISTN bin to reduce influences from attention switch costs (see Section 3.1). As for the behavioral analysis, we performed a linear trend analysis between the AMI as a function of ISTN bin, but found no significant effects in the grand average ($F(6, 114) = 0.2830$, $p = 0.94$). In the grand average alpha-modulation topography (Fig. 4B) we found mainly left hemispheric modulation; however the left hemisphere AMI (AMI_L) did not systematically change with ISTN either ($F(6, 114) = 0.955$, $p = 0.46$). We additionally tested whether resetting the ISTN (see Materials and methods section) after an incorrect response to a repeat trial might have caused the lack of significant effects in the grand average. The ISTN resets could potentially have introduced variability into subjective probabilities. To do so, we again conducted the linear trend analysis of the alpha modulation index with ISTN bins, but removed blocks of trials with errors to repeat trials. The trend remained non-significant ($F(6, 114) = 0.4973$, $p = 0.81$). Importantly, we observed that the ability to detect the implicit likelihood of events strongly differed across participants. We computed the switch-rate for each ISTN bin and all subjects. Then, we correlated the switch-rate per ISTN bin with the switch-trial likelihood per ISTN bin (see Fig. 2) for each subject.

Table 1
Number of trials after artifact rejection per ISTN bin.

ISTN bin	Total number of trials	Trials, attention left	Trials, attention right
1	111.5 ± 17.9	55.3 ± 9.5	56.3 ± 9.1
2	112.8 ± 17.8	55.4 ± 8.6	57.5 ± 10.0
3	109.3 ± 18.7	54.7 ± 9.6	54.6 ± 10.2
4	96.5 ± 18.6	47.6 ± 9.4	48.9 ± 10.0
5	73.0 ± 14.1	35.8 ± 7.6	37.2 ± 7.5
6	51.4 ± 14.1	23.9 ± 6.7	27.5 ± 6.0
7	36.3 ± 11.3	17.2 ± 4.4	19.1 ± 5.0

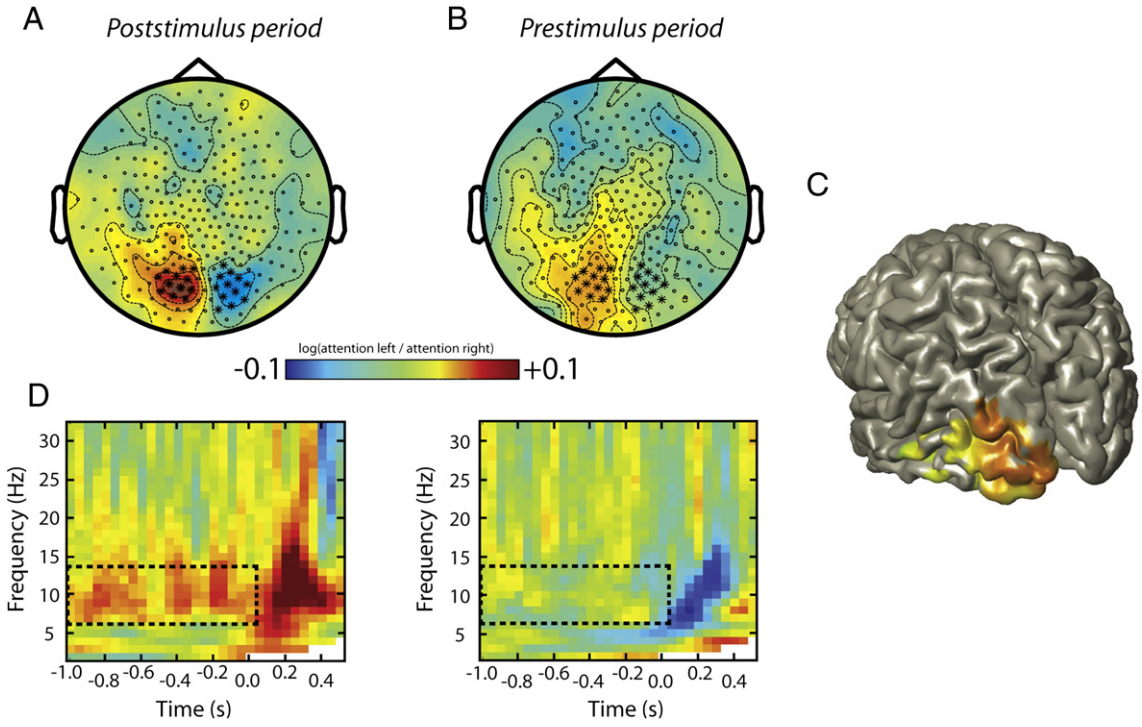

Fig. 4. Alpha modulation and ROI selection. All plots show the contrast of attention left versus right repeat trials; grand-average. A Topographic map of stimulus-induced alpha-band (7–13 Hz) modulation for all repeat trials ($t = 0$ to 0.5 s). The twelve most sensitive sensors on the left and on the right hemisphere in the induced alpha-band response were selected for further analysis (marked with asterisks). B Topographic map of prestimulus alpha-band modulation for all repeat trials ($t = -1$ to 0 s). C Source reconstruction of the prestimulus alpha (7–13 Hz) modulation ($t = -1$ s to 0 s). Only the significant cluster from the permutation test is depicted ($p < 0.05$). D Time–frequency representation of power of the alpha modulation for the left and the right ROIs, respectively. The box (dotted lines) shows the frequency range chosen for A, B and C and the chosen prestimulus interval for all further analyses as well as for B and C.

Next, we built the 95%-confidence interval (CI) around the mean of all correlation coefficients and investigated how many correlation coefficients were outside this interval. The confidence interval ranged from −0.09 to 0.45. We found eight subjects with a correlation coefficient below the lower bound of the CI and ten subjects with a correlation coefficient above the upper bound of the CI. Due to the wide spread of correlation coefficients, we concluded that there were large inter-individual differences in behaviorally adjusting to the parameters of the task.

Next, we asked whether the behavioral adjustment can be explained by an adjustment of posterior alpha modulation. To quantify this, we computed for each subject the regression slopes of the behavioral performance and of the AMI with respect to ISTN bins. We hypothesized that subjects with a more pronounced behavioral task adjustment (i.e. a better ability to detect switch trials) also adapted their alpha activity to the properties of the task. In other words, we expected a significant negative inter-subject correlation of these two regression slopes (better task performance should result in more attention to the unattended hemifield, thus a weaker AMI). The regression slope–slope correlation analysis revealed that an adaptation of the AMI to the task statistics does have these behavioral effects. Fig. 5A shows the slope of switch-rate (y-axis) as a function of the slope of the alpha modulation index (x-axis) revealing a significant negative correlation ($r^2 = 0.3096$, $p = 0.01$). The change in switch-rate is not explained by individual differences in speed-accuracy trade-off because there was no significant correlation between slope of AMI and reaction time for switch trials ($r^2 = 0.0190$, $p > 0.5$, Fig. 5B). For repeat trials, we did not find significant correlations, neither for the slope of the correct response rate ($r^2 = 0.0909$, $p > 0.1$) nor for the slope of reaction times ($r^2 = 0.0056$, $p > 0.7$). Also the number of ISTN resets per subject was not correlated with the switch rate slope ($r^2 = 0.0803$, $p > 0.2$) or with the AMI slope ($r^2 = 0.1429$, $p > 0.1$). The result remained significant when we included the AMI data from the first ISTN bin (switch-rate: $r^2 = 0.2098$, $p = 0.04$), while reaction times to switch trials stayed not significant (switch trials RT: $r^2 = 0.0082$, $p > 0.7$). Also for repeat trials, results stayed not significant when including the first ISTN bin (correct response rate to repeat trials: $r^2 = 0.0264$, $p > 0.4$; repeat trial RT: $r^2 = 0.0255$, $p > 0.5$). In short, this analysis demonstrates that subjects that adapted their alpha modulation according to the task statistics also detected more switch trials with increasing ISTN. Likewise, subjects that did not adapt the alpha modulation got worse at detecting the switch trials with increasing ISTN.

Discussion

In a covert attention switching paradigm, we have investigated how subjects adapt to statistical properties of the environment; here a linear increase in the likelihood of stimuli prompting a switch in spatial attention. We found individual differences in how subjects adjusted behaviorally to the increase in switch trial likelihood. Interestingly, the individual degree of adjustment of posterior alpha band lateralization to switch trials likelihood predicted how well subjects adjusted their behavior. We conclude that anticipatory alpha band lateralization reflects the allocation of spatial attention as modulated by the implicit statistical properties of the environment.

The posterior alpha rhythm reflects the state of anticipatory visual attention

Recent studies have shown that alpha power is modulated in anticipation of upcoming stimulus (e.g. Bonnefond and Jensen, 2012; Rohenkohl and Nobre, 2011; Thut et al., 2006; van Ede et al., 2012; Worden et al., 2000). Two recent studies suggest that this anticipatory alpha rhythm is modulated according to properties of the environment in both the visual and the somatosensory system (Gould et al., 2011; Haegens et al., 2011). In both studies, there was significantly stronger hemispheric alpha lateralization for highly reliable as compared to

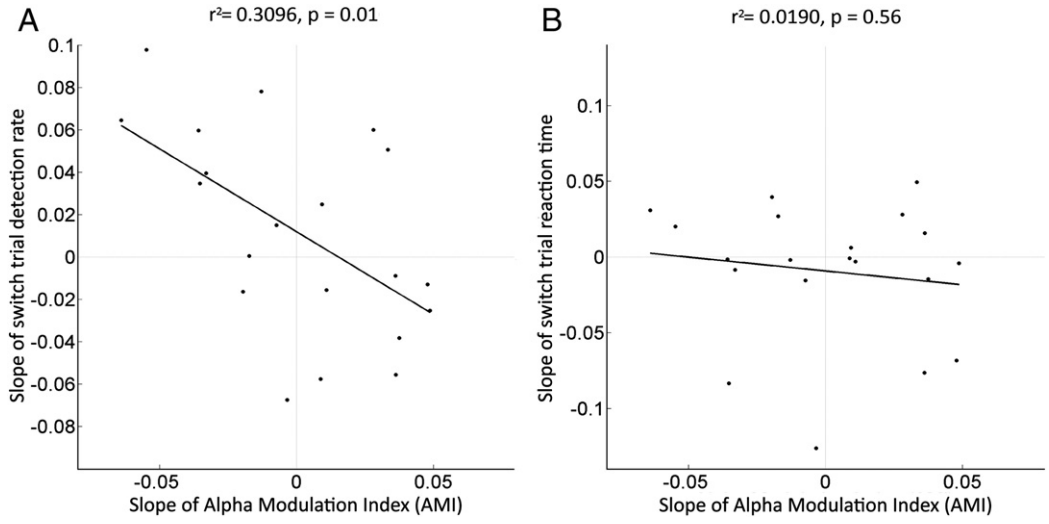

Fig. 5. Regression slope–slope correlations across subjects when relating the AMI to behavioral measures. A Correlation of AMI slopes and switch-rate slopes. The slopes of switch-rate correlated strongly with the slopes of the AMI ($r^2 = 0.3096$, $p = 0.01$). A subject with a negative AMI slope and a positive switch-rate slope suggests that this subject adjusts to the implicit change in switch trial likelihood. A subject with the opposite pattern (positive AMI slope and a negative switch-rate slope) suggests that this subject did not adjust properly to the implicit change in switch trial likelihood. Thus, subjects that adapted their AMI to the task statistics were also those who got better in switching with increasing ISTN. B Correlation of AMI slopes and switch-trial reaction time slopes. There was no significant correlation between AMI slopes and slopes of switch trial reaction time ($r^2 = 0.0190$, $p > 0.5$).

unreliable cues. Complementary to these earlier reports, we show that top-down modulation of posterior alpha power does not require explicit knowledge about stimulation likelihood. Instead, the brain adapts implicitly to statistical properties of the environment which then is reflected in the spatial distribution of alpha power preceding the stimulus. Crucially, we found that the strength of pre-stimulus alpha power predicted the magnitude of behavioral adjustment in individual subjects. This demonstrates that subjects who manage to adjust alpha power lateralization appropriately to the statistics of the environment are able to optimize their individual behavioral performance.

In the grand average of the prestimulus interval, we found a significant modulation over the left hemisphere but not over the right hemisphere. In the somatosensory domain, a similar effect has been found for uninformative spatial cues during a covert attention task (Haegens et al., 2011). In the visual domain, this difference between the left and right hemisphere is consistent with the classical visuospatial model of Heilman and van den Abell (1980) that posits that left parietal regions process right hemifield visual input, whereas right parietal regions process both hemifields (reviewed in Sack, 2009). As such the model predicts that the left hemisphere will be more strongly modulated than the right when spatial attention is changed between hemifields. This notion is directly supported by a TMS study that perturbed either the left or right inferior parietal sulci (IPS) and then characterized the prestimulus alpha-band activity in a covert attention task (Capotosto et al., 2012). They found that interfering with the right IPS resulted in a bilateral increase in anticipatory alpha-band power over occipital cortex and consequent performance deficits, whereas stimulation of left IPS did not. Similarly, Sauseng et al. (2011) used TMS to perturb the left and right FEF and found that only disturbing the right FEF reduces frontoparietal coupling in the alpha-band and impairs performance during visual spatial attention shifting. Thus, the right hemisphere might have a more global contribution during allocation of spatial attention, which explains the lack of modulation over the right hemisphere when contrasting attention to the left versus right hemifield.

Behavioral performance, stimulus intensity and motivation

We found a significant correlation between posterior alpha power and performance in terms of attention switching. It is important to note that subjects were encouraged to prioritize accuracy over reaction times (RTs). This could explain why alpha power and reaction times did not correlate in contrast to previous reports (e.g. Gould et al., 2011; Kelly et al., 2009; Thut et al., 2006). We did however demonstrate a relation between performance and the ability to modulate prestimulus alpha power. In particular we found that the individual degree of alpha adjustment was correlated with performance changes. This difference could be explained by some subjects relying on detecting the stimulus driven appearance of switch trials rather than on the statistics of switch-stimuli likelihood. In our paradigm, stimulus intensities were individually adjusted for each subject (see Section 2.2). To test if differences in stimuli intensity explained the effects, we asked whether the relative difference in intensity between the neutral and the colored stimulus was correlated with the AMI slope or switch-rate slope over ISTN but this was not the case for the AMI slope ($r^2 = 0.0703$, $p > 0.2$) nor for the switch-rate slope ($r^2 = 0.0575$, $p > 0.3$). Another possible explanation might be that subjects who did not adjust the hemispheric alpha lateralization according to target likelihood did not understand the task or were less motivated. This would imply that non-adaptive subjects had worse performance. We therefore tested whether subjects with a positive AMI slope over ISTNs had a lower detection rate of repeat trials than subjects with a negative AMI slope; however, this was not the case ($t(18) = -1.1212$, $p > 0.2$). A similar analysis considering the switch-rate also showed no significance ($t(18) = -0.695$, $p > 0.5$). Thus while some subjects were better able at adapting to the implicit task design, this was not explained by differences in behavioral performance or by motivational factors.

Which networks might control the posterior alpha power?

We have shown that posterior alpha power is modulated in a top-down manner by incorporating implicit statistical knowledge about the environment. Direct top-down control on visual attention most likely stems from the frontal eye fields (FEF) via the intraparietal sulcus (IPS), which are part of the dorsal attention network (see Corbetta and Shulmann, 2002; Kastner and Ungerleider, 2000). Capotosto et al. (2009) used transcranial magnetic stimulation (TMS) to perturb the FEF and IPS during the preparation interval in a covert attention paradigm. They found that this perturbation not only impaired detection performance, but also the task-modulated parieto-occipital alpha-band power. This study indicates that FEF and IPS are causally involved in the control of posterior alpha-band power.

Apart from neocortical connections, the FEF are also strongly connected to subcortical regions such as the superior colliculus (SC) (reviewed in Hikosaka et al., 2000; Munoz and Everling, 2004). Beside its involvement in saccade preparation and execution, the SC is sensitive to behaviorally important, salient events (Comoli et al., 2003; see Boehnke and Munoz, 2008 for a review) and is therefore likely to be engaged in subjects performing our paradigm. Furthermore, both the SC and the FEF are strongly connected to the basal ganglia (Hikosaka et al., 2000; Neggers et al., 2012). In a recent fMRI study, van Schouwenburg et al. (2010) found that the BOLD signal in the basal ganglia (BG) increased when a visual stimulus successfully produced a switch in visual attention. Thus, the BG is likely to be part of the network engaged in the current study. van Schouwenburg et al. (2010) also found strong modulation of the inferior frontal gyrus (IFG) in response to salient stimulation changes. Further investigations are required to study the involvement of above mentioned regions and to establish the link between fronto-striatal networks and posterior networks. For such investigations, animal electrophysiology or fMRI recordings might be more sensitive than MEG recording due to their high spatial resolution.

Conclusion and future work

We found that anticipatory spatial attention is reflected in the distribution of posterior alpha band power which is predictive of individual detection performance in response to environmental task statistics. The hypothesis that alpha power reflects the anticipatory attention state of the subject could be applied in neurofeedback paradigms. Recently it has been shown that ADHD patients show a lack of sustaining a high degree of alpha lateralization (ter Huurne et al., 2013). A neurofeedback paradigm could aim at optimizing the subject's awareness of their state of attention by providing online feedback using a measure reflecting the posterior alpha power lateralization. This could be used in setup directly training the subjects' ability to modulate their alpha band activity.

Acknowledgments

M.B. is supported by the Fyssen Foundation. R.C. was supported by a Human Frontiers Science Program grant to Kae Nakamura, Nathaniel Daw and R.C. under grant number RGP0036/2009-c, as well as a VIDI grant from the Innovational Research Incentives Scheme of the Netherlands Organisation for Scientific Research (NWO) under grant number 016-095-340 and a James McDonnell scholar award. She has been a consultant to Abbott Laboratories and Pfizer, but she is not an employee or a stock shareholder. O.J. is supported by the research program “The healthy brain” funded by the Netherlands Initiative Brain and Cognition (NIHC), a part of the Organization for Scientific Research (NWO) under grant number 056-14-011 and by a VICI grant under number 453-09-002.

References

Bastiaansen, M.C., Knösche, T.R., 2000. Tangential derivative mapping of axial MEG applied to event-related desynchronization research. Clin. Neurophysiol. 111, 1300–1305.
Boehnke, S.E., Munoz, D.P., 2008. On the importance of the transient visual response in the superior colliculus. Curr. Opin. Neurobiol. 18 (6), 544–551.
Bonnefond, M., Jensen, O., 2012. Alpha oscillations serve to protect working memory maintenance against anticipated distracters. Curr. Biol. 22, 1969–1974.
Capotosto, P., Babiloni, C., Romani, G.L., Corbetta, M., 2009. Fronto-parietal cortex controls spatial attention through modulation of anticipatory alpha rhythms. J. Neurosci. 29, 5863–5872.
Capotosto, P., Babiloni, C., Romani, G.L., Corbetta, M., 2012. Differential contribution of right and left parietal cortex to the control of spatial attention: a simultaneous EEG-rTMS study. Cereb. Cortex 22 (2), 446–454.
Comoli, E., Coizet, V., Boyes, J., Bolam, J.P., Cantera, N.S., Quirk, R.H., Overton, P.G., Redgrave, P., 2003. A direction projection from superior colliculus to substantia nigra for detecting salient visual events. Nat. Neurosci. 6 (9), 974–980.
Corbetta, M., Shulman, G.L., 2002. Control of goal-directed and stimulus-driven attention in the brain. Nat. Rev. Neurosci. 3 (3), 201–215.
Foxe, J.J., Snyder, A.C., 2011. The role of alpha-band brain oscillations as a sensory suppression mechanism during selective attention. Front. Psychol. 2, 154.
Gould, I.C., Rushwort, M.F., Nobre, A.C., 2011. Indexing the graded allocation of visuospatial attention using anticipatory alpha oscillations. J. Physiol. 105 (3), 1318–1326. http://dx.doi.org/10.1152/jn.00653.2010.
Gross, J., Kujala, J., Hämäläinen, M., Timmermann, L., Schnitzler, A., Salmelin, R., 2001. Dynamic imaging of coherent sources: studying neural interactions in the human brain. Proc. Natl. Acad. Sci. U. S. A. 98, 694–699.
Haegens, S., Händel, B., Jensen, O., 2011. Top-down controlled alpha band activity in somatosensory areas determines behavioural performance in a discrimination task. J. Neurosci. 31 (14), 5197–5204. http://dx.doi.org/10.1523/JNEUROSCI.5199-10.2011.
Händel, B.F., Haarmeiert, T., Jensen, O., 2011. Alpha oscillations correlated with detected inhibition of unattended stimuli. J. Cogn. Neurosci. 23 (9), 2494–2502. http://dx.doi.org/10.1162/jocn.2010.21557.
Heilman, K.M., van den Abell, T., 1980. Right hemisphere dominance for attention: the mechanism underlying hemispheric asymmetries of inattention (neglect). Neurology 30 (3), 327–330.
Hikosaka, O., Takikawa, Y., Kawagoe, R., 2000. Role of the basal ganglia in the control of purposive saccadic eye movements. Physiol. Rev. 80 (3), 953–978.
Jensen, O., Mazaheri, A., 2010. Shaping functional architecture by oscillatory alpha activity: gating by inhibition. Front. Hum. Neurosci. 4 (186).
Jensen, O., Bonnefond, M., VanRullen, R., 2012. An oscillatory mechanism for prioritizing salient unattended stimuli. Trends Cogn. Sci. 16 (4), 200–206.
Kastner, S., Ungerleider, L.G., 2000. Mechanisms of visual attention in the human cortex. Annu. Rev. Neurosci. 23, 315–341.
Kelly, S.P., Gomez-Ramirez, M., Foxe, J.J., 2009. The strength of anticipatory spatial biasing predicts target discrimination at attended locations: a high-density EEG study. Eur. J. Neurosci. 30, 2224–2234. http://dx.doi.org/10.1111/j.1460-9568.2009.06980.x.
Klimesch, W., 1999. EEG alpha and theta oscillations reflect cognitive and memory performance: a review and analysis. Brain Res. Brain Res. Rev. 29 (2–3), 169–195.
Klimesch, W., 2012. α-Band oscillations, attention, and controlled access to stored information. Trends Cogn. Sci. 16 (12), 606–617. http://dx.doi.org/10.1016/j.tics.2012.10.007.
Maris, E., Oostenveld, R., 2007. Nonparametric statistical testing of EEG- and MEG-data. J. Neurosci. Methods 164 (1), 177–190.
Monsell, S., 2003. Task switching. Trends Cogn. Sci. 7 (3), 134–140.
Munoz, D.P., Everling, S., 2004. Look away: the anti-saccade task and the voluntary control of eye movement. Nat. Rev. Neurosci. 5 (3), 218–228.
Neggers, S.F.W., van Diepen, R.M., Zandbelt, B.B., Vink, M., Mandl, R.C.W., et al., 2012. A functional and structural investigation of the human fronto-basal volitional saccade network. PLoS ONE 7 (1), e29517. http://dx.doi.org/10.1371/journal.pone.0029517.
Nolte, G., 2003. The magnetic lead field theorem in the quasi-static approximation and its use for magnetoencephalography forward calculation in realistic volume conductors. Phys. Med. Biol. 48, 3637–3652.
Oostenveld, R., Fries, P., Maris, E., Schoffelen, J.M., 2011. FieldTrip: open source software for advanced analysis of MEG, EEG, and invasive electrophysiological data. Computational Intelligence and Neuroscience. http://dx.doi.org/10.1155/2011/156869 (2011).
Percival, D.B., Walden, A.T., 1993. Spectral Analysis for Physical Applications: Multitaper and Conventional Univariate Techniques. Cambridge UP, Cambridge, UK.
Rohenkohl, G., Nobre, A.C., 2011. Alpha oscillations related to anticipatory attention follow temporary expectations. J. Neurosci. 31 (40), 14076–14084.
Romei, V., Gross, J., Thut, G., 2010. On the role of prestimulus alpha rhythms over occipito-parietal areas in visual input regulation: correlation or causation? J. Neurosci. 30 (25), 8692–8697.
Rubner, Y., Tomasi, C., Guibas, L.J., 1998. A metric for distributions with applications to image databases. ICCV 59–66 (1998).
Ruzon, M., Tomasi, C., 1999. Color edge detection with the compass operator. CVPR 160–166 (1999).
Sack, A.T., 2009. Parietal cortex and spatial cognition. Behav. Brain Res. 202, 153–161.
Sauseng, P., Klimesch, W., Stadler, W., Schabus, M., Doppelmayr, M., Hanslmayr, S., Gruber, W.R., Birbaumer, N., 2005. A shift of visual spatial attention is selectively associated with human EEG alpha activity. Eur. J. Neurosci. 22, 2917–2926.
Sauseng, P., Feldheim, J.F., Freunberger, R., Hummel, F.C., 2011. Right prefrontal TMS disrupts interregional anticipatory EEG alpha activity during shifting of visuospatial attention. Front. Psychol. 2 (241). http://dx.doi.org/10.3389/fpsyg.2011.00241.
Schoffelen, J.M., Oostenveld, R., Fries, P., 2008. Imaging the human motor system's beta-band synchronization during isometric contraction. Neuroimage 41, 437–447.
Stolk, A., Todorovic, A., Schoffelen, J.M., Oostenveld, R., 2013. Online and offline tools for head movement compensation in MEG. Neuroimage 68, 39–48.
ter Huurne, N., Onnink, M., Kan, C., Franke, B., Buitelaar, J., Jensen, O., 2013. Behavioral consequences of aberrant alpha lateralization in attention deficit/hyperactivity disorder. Biol. Psychiatry 75 (4), 227–233.
Thut, G., Nietzel, A., Brandt, S.A., Pascual-Leone, A., 2006. Alpha-band electroencephalographic activity over occipital cortex indexes visuospatial attention bias and predicts visual target detection. J. Neurosci. 26 (37), 9494–9502.
van Ede, F., Köster, M., Maris, E., 2012. Beyond establishing involvement: quantifying the contribution of anticipatory α- and β-band suppression to perceptual improvement with attention. J. Neurophysiol. 108 (9), 2362–2452.
van Schouwenburg, M.R., den Ouden, H.E.M., Cools, R., 2010. The human basal ganglia modulate frontal-posterior connectivity during attention shifting. J. Neurosci. 30 (29), 9910–9918.
Worden, M.S., Foxe, J.J., Wang, N., Simpson, G.V., 2000. Anticipatory biasing of visuospatial attention indexed by retinotopically specific alpha-band electroencephalography increases over occipital cortex. J. Neurosci. 20 (6) (RC 63).